CFSRC COLLOQUIUM

Proceedings of the Cold-Formed Steel Research Consortium Colloquium
20-22 October 2020 (cfsrc.org)

Impact of gravity detailing on the thermal performance of cold-formed steel wall assemblies

Divyansh R. Kapoor[1], Kara D. Peterman[2]

Abstract

Considering building thermal performance in addition to structural performance is paramount to sustainable design. Structural systems bleed heat from interior to exterior through thermal bridges, structural elements that either span the building envelope or dramatically reduce the efficiency of insulating components. Materials that have high thermal conductivities are particularly susceptible to forming thermal bridges; steel has a relatively high thermal conductivity compared to other building materials and demands attention. In cold-formed steel buildings, repetitively framed studs act as thermal bridges. As typical interior insulation is placed in the wall cavity, between wall studs, the studs impact the effectiveness of the insulation layer. This work aims to characterize and quantify the impact of design choices on the thermal performance of exterior structural cold-formed steel walls. This is accomplished via three-dimensional finite element modeling. First the models are validated against existing experimental and computational efforts, then expanded to capture a suite of common detailing. Stud thickness, web depth, and spacing are the focus of this paper. A range of climate zones (corresponding to continuous insulation thickness and cavity insulation R-value) are also explored. The results suggest that web depth does not impact thermal performance while stud thickness and spacing do contribute to the total energy lost through the structural system. This paper formulates recommendations to designers regarding cross-section selection and exterior wall detailing.

1. Introduction

Repetitively framed cold-formed steel (CFS) walls are susceptible to the phenomenon of thermal bridging due to the high relative conductivity of steel with respect to its surrounding components. The CFS members offer a path of least resistance for energy to flow through the wall assembly causing a myriad of problems like reduced thermal performance, condensation issues, and occupant discomfort. The problem of thermal bridging in CFS walls is well known and the focus of bulk of existing literature is on mitigation strategies and overall wall performance.

Previous work by Martins et al [1] have investigated the effectiveness of available thermal mitigation strategies such as slotted steel profiles, vacuum insulated panels (VIPs), rubber strips, and polyurethane (PU) foam. The parametric study focused on single and combination mitigation strategies and it was found that a combination of slotted steel profiles, VIPs, rubber strips, and bolted connections provided the highest reduction in U-value of 68%.

Recent works conducted by Morrison Hershfield [2] for the American Iron and Steel Institute (AISI) have focused on parametrically studying overall thermal performance of archetype wall assemblies via three-dimensional steady state analysis and benchmarked finite element models. The key parameters for this study were CFS member depth, cavity insulation, external continuous insulation (CI), and fastener patterns. It was determined that stud depth and fastener patterns have negligible impact on heat flow, but cavity insulation and CI drastically changed the thermal performance. However, this research project does not aim to address individual component level contributions to thermal performance. Rather, it is a holistic view of the thermal performance of the complete wall assembly.

Component level thermal performance was analyzed by the authors in AISI RP19-2 [3]. A parametric evaluation comprising of eighty unique assemblies were evaluated using ISO 10211 [4] conforming specialty heat transfer software Heat3. The key parameters of this study were CFS member gage, spacing, depth, external continuous insulation R-value, and fastener patterns. Thermal performance was measured by means of overall heat flow and component thermal transmittance values and trends in the same were reported. The results indicated that CFS detailing can significantly alter the thermal performance of

[1] Graduate Research Assistant, Department of Civil & Environmental Engineering, University of Massachusetts, Amherst, dkapoor@umass.edu
[2] Assistant Professor, University of Massachusetts, Amherst, kdpeterman@umass.edu

wall assemblies. Additionally, it was also observed that trends in CFS member impact on overall heat flow and thermal transmittance coefficient can be utilized to estimate thermal performance and make design choices that minimize impact of thermal bridging.

In this paper, trends observed in AISI RP19-2 [3] are further examined to aid in reduction of thermal bridging loses during the gravity detailing phase of design. Sixteen unique assemblies differing in CFS member spacing, depth, and gage are evaluated in conjunction with variable external continuous insulation. The CFS parameters are representative of typical CFS detailing in the North American industry and insulation combinations are based on building envelope requirements for different ASHRAE 90.1 [5] climate zones. Based on the results of this parametric evaluation, guidance is provided on gravity detailing by presenting impact of detailing decisions such as increasing gage, cross sectional depth, and spacing. Further, methods of modifying heat flows and estimating thermal performance due to some detailing choices are also presented.

2. Representative wall assembly

The representative wall assembly (Refer Figure 1) was adapted from previous works by the authors [AISI RP19-2 [3] and is based on the wall assemblies studied in AISI RP18-1 [2].

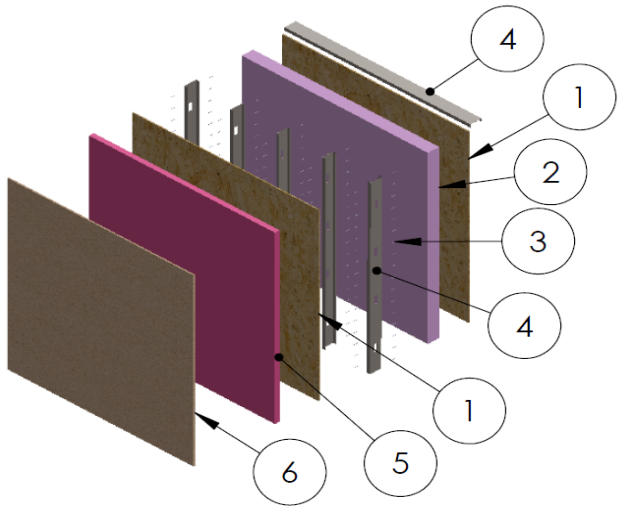

Figure 1: Representative Wall Assembly Components: 1—Gypsum board (Sheathing); 2—Cavity Insulation; 3—Fasteners; 4—CFS Studs and Tracks (Bottom track not shown for clarity); 5—XPS; 6—Stucco

It comprises of a 2440 mm (8 ft) by 2440 mm (8 ft) cold-formed steel (CFS) wall panel with variable stud depth, spacing, and member thickness. The studs are bounded by CFS tracks on either ends and stiffening bridging is located 865 mm (36 in) above the bottom track. The CFS frame is filled with fiberglass batt insulation and is covered on both sides with 16 mm (5.8 in) thick gypsum sheathing. External continuous insulation (CI) varying between 38.1 mm (1.5 in) and 63.5 mm (2.5 in) in thickness is present wherever applicable. The exterior surface is covered with 19 mm (3/4 in) thick stucco, and all attachments are made with self-drilling self-tapping screws. The overall thickness of the wall assembly varies from 142.9 mm (5.625 in) to 266.7 mm (10.50 in) and is dependent on CFS member depth and CI thickness

3. Parametric evaluation

Parameters (Refer Table 1) were selected to study trends in thermal performance due to varying structural detailing such as CFS member depth, gage (thickness), and spacing. Hence two CFS member depths, 93 mm (3.625 in) and 153 mm (6.000 in), were investigated in combination with five thicknesses (0.84 mm to 2.47 mm) and two spacing options [407 mm (16 in) and 610 mm (24 in)].

Table 1: Summary of Parametric Evaluation

Parameter	Variable Values	Applicable Assemblies
Sheathing Type and Thickness (1)	Gypsum - 15.8 mm (5/8 in)	All
Cavity Insulation R - Value (2)	2.29 m^2·K/W (R-13)	All
Fastener Diameter and Length (3)	#6 Fastener (Sheathing to CFS)	All
CFS Member Depth (4)	93 mm (3.625 in)	PA 1 - 4 & PA 9 - 10
	153 mm (6.000 in)	PA 5 - 8, PA 11 - 12, & PA 13 - 16
External Insulation R - Value (5)	1.33 m^2·K/W (R-7.5)	PA - 2, 6, 10, & 12
	1.77 m^2·K/W (R-10.0)	PA - 3 & 7
	2.21 m^2·K/W (R-12.5)	PA - 4 & 8
Exterior Finish and Thickness (6)	Stucco - 19 mm (3/4 in)	All
CFS Stud Spacing	407 mm (16 in)	PA 1 - 8 & PA 13 - 16
	610 mm (24 in)	PA 9 - 12
CFS Member Thickness	0.84 mm (33 mil)	PA 13
	1.09 mm (43 mil)	PA 01 - PA 12
	1.37 mm (54 mil)	PA 14
	1.73 mm (68 mil)	PA 15
	2.47 mm (97 mil)	PA 16

Additionally, the impact of continuous insulation (CI) was also investigated by varying external insulation between 38.1 mm (1.5 in) thick 1.33 m^2·K/W (R-7.5) and 63.5 mm

(2.5 in) thick 2.21 m²·K/W (R-12.5) external CI. This CI in combination with 2.29 m²·K/W (R-13) cavity insulation meet the minimum building envelope requirements based on ASHRAE 90.1 [5] Tables 5.5-0 through 5.5-7 and are representative of climate zones (CZ) 0 through 7. Sixteen unique wall assemblies were evaluated, and the parametric evaluation has been summarized in Table 1.

4. 3-D steady-state analysis and validation

Finite element models of the wall assemblies were created and analyzed in ISO 10211 [4] conforming specialty heat transfer software Heat 3. Due to linear geometry modelling restrictions in Heat 3 version 08 [6], CFS member corner radii were simplified as right-angle intersections and fasteners were modelled as cuboids with cross-sectional area equal to the area of the fastener shaft. Material properties used for the analysis are consistent with Section A3.3.1 of ASHRAE 90.1 [5] and have been summarized in Table 2.

Surface boundary conditions were applied to the wall assemblies in Heat3 in the form of air film convective coefficients and a non-dimensionalized temperature index. Air film convective coefficients were based on Table 10, Chapter 26 of ASHRAE HoF [7] and a non-dimensionalized temperature index was used to make the solutions applicable to any temperature range. The exterior surface of the wall assembly was exposed to a temperature of 0°C (32.0 °F) and surface film coefficient of 34.1 W/m²·°C (6.00 BTU/hr·ft² ·°F). The interior surface was exposed to a temperature of 1°C (33.8 °F) and a surface film coefficient of 8.31 W/m²·°C (1.46 BTU/hr·ft²·°F).

Validation of modelling assumptions, material properties, and boundary conditions was done by comparing Heat3 simulated U-value and R-value with previously published values in AISI RP18-1 [2]. The modelling approach used in AISI RP18-1 [2] was validated against reference cases from ASHRAE 785 RP [8], ASHRAE 1365–RP [9], and ORNL hotbox compilation study [10]. Four wall assemblies were modelled in Heat3 for methodology validation. Simulated values from Heat3 were within 3% and -3% of published R-values and U-values respectively, and the modelling methodology was deemed validated. These results are presented in detail in AISI RP19-2 [3].

Table 2: Material properties used for the 3-D steady-state analysis

Material	Thickness	Conductivity K-Value	Component R-Value
	m (in)	W/m·K (BTU-in/hr·ft² °F)	m²·K/W (hr·ft² °F /BTU)
Stucco	0.0191 (0.75)	1.36 (9.38)	0.02 (0.08)
Gypsum	0.0159 (0.625)	0.17 (1.11)	0.1 (0.563)
33 Mil Steel	0.0009 (0.0329)	71.4 (495)	-- (--)
43 Mil Steel	0.0011 (0.0428)	71.4 (495)	-- (--)
54 Mil Steel	0.0014 (0.0538)	71.4 (495)	-- (--)
68 Mil Steel	0.0018 (0.0677)	71.4 (495)	-- (--)
97 Mil Steel	0.0025 (0.0966)	71.4 (495)	-- (--)
R-13	0.0921 (3.625)	0.05 (0.279)	2.29 (13)
R-13	0.1524 (6.000)	0.07 (0.462)	2.29 (13)
R - 7.5	0.0381 (1.5)	0.029 (0.200)	1.32 (7.50)
R - 10.0	0.0508 (2.0)	0.029 (0.200)	1.76 (10.0)
R - 12.5	0.0635 (2.5)	0.029 (0.200)	2.20 (12.5)

5. Quantification of thermal transmittance coefficients

Linear thermal transmittance coefficients for the CFS members were calculated by comparing heat flows obtained from Heat 3 through iterations of the same assembly. First, clear wall heat flow value, Q_{CW}, was estimated from the 3-D steady-state analysis. Then the contribution of thermal anomalies was indirectly measured by removing the anomaly and comparing the new heat flow ($Q_{No\ Studs}$, and $Q_{No\ Tracks}$) with Q_{CW}. Equation 1 and 2 were used to estimate the linear transmittance coefficients of studs and tracks, respectively.

$$\psi_{Studs} = \frac{Q_{cw} - Q_{No\ Studs}}{L_{Studs}} \quad (1)$$

$$\psi_{Tracks} = \frac{Q_{cw} - Q_{No\ Tracks}}{L_{Tracks}} \quad (2)$$

6. Impact of CFS member gage

CFS member gage directly impacts the heat flow through the wall assembly and its components. Five CFS member thickness were evaluated, and heat flow increased by 17% when comparing 0.84 mm (33 mil) with 2.47 mm (97 mil) assemblies. The corresponding increase in heat flow through studs and tracks was 42% and 21% respectively.

The increase in heat flow is non-linear (Refer Figure 2) and an empirical relationship (Refer Equation 3) was derived that can predict heat flow values within 3% of FEA (Heat3) values for assemblies with the same stud depth and spacing as the reference case. In Equation 3, Q1 and Q2 are the reference and unknown heat flow values, T1 and T2 are the CFS member thicknesses, and K is the stud depth and spacing factor of **1.049** for 153 mm (6.000 in) CFS studs spaced at 407 mm (16 in) on center.

$$Q_2 = Q_1(K)^{(\frac{T_2}{T_1})} \quad (3)$$

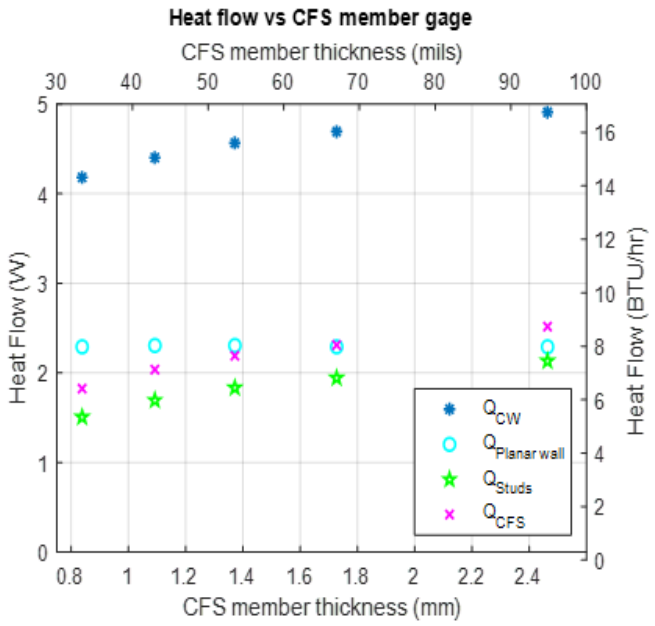

Figure 2: Summary of heat flow by component vs CFS member thickness

This equation was further validated by modifying and comparing heat flow values with previously studied assemblies in AISI RP19-2 and the predictions were within 6% of Heat3 values when CI was present. This error was less than 1% when no CI was present. Hence, known heat flow values can be empirically modified to account for any change in gage provided other assembly configurations remain unchanged.

7. Impact of CFS stud spacing

Reducing stud spacing from 610 mm (24 in) to 407 mm (16 in) on center increases the heat flow through the studied assemblies by 13% when no external continuous insulation is present. This increase in heat flow reduces to 7% when a 1.33 m²·K/W (R-7.5) layer of external continuous insulation (CI) is added. Further, previous works by the authors have found that this increase reduces to 5% when 2.21 m²·K/W (R-12.5) CI is present [3]. Impact of stud spacing is significant but reduces when continuous insulation is added.

Reducing stud spacing also increased the thermal transmittance coefficient of studs (ψ_{stud}) but decreased the same for tracks (ψ_{track}). ψ_{Stud} and ψ_{track} increased and decreased by 2% and 5% respectively for no CI assemblies. The cumulative effect of change in transmittance coefficients was a 13% increase in heat flow. When a 1.33 m²·K/W (R-7.5) layer CI was present, ψ_{Stud} and ψ_{track} increased and reduced by 3% and 12% respectively for a net change of 7% in the overall heat flow when spacing was reduced.

It was also observed that the linear thermal transmittance coefficients estimated for 610 mm (16 in) on center assemblies can accurately predict heat flow values for 407 mm (24 in) on center assemblies and vice versa with a net error of less than 2% (Refer Table 3).

Table 3: Summary of predicted vs simulated heat flows

Stud Depth	R_{CI}	$\psi_{studs,16}$	$\psi_{tracks,16}$	$Q_{pred,24}$	$Q_{Heat3,24}$	Δ
	m²·K/W	W/m·K		W		%
93 mm (3.625 in)	No XPS	0.104	0.072	3.915	3.949	0.9
	1.33	0.027	0.014	1.926	1.946	1.0
153 mm (6.000 in)	No XPS	0.099	0.073	3.875	3.895	0.5
	1.33	0.027	0.016	1.939	1.961	1.1

8. Impact of CFS member depth

Increasing stud depth from 93 mm (3.625 in) to 153 mm (6.000 in) has negligible (<2%) impact on overall heat flow through the wall assembly. Presence of continuous insulation completely mitigates the negligible impact increasing stud depth has on overall heat flow. This result is consistent with trends in heat flow observed in AISI RP18-1 [2] where assemblies with 88.9 mm (3.5 in), 254.0 mm (10 in) and 304.8 mm (12 in) studs were evaluated.

93 mm (3.625 in) stud depth thermal transmittance coefficients were used to predict heat flow values for 153 mm (6.000 in) stud depth assemblies. The predicted values were within 2% (Refer Table 4) of the 3-D steady state finite element simulation values for both 407 mm (16 in) and 610 mm (24 in) assemblies. This validates the applicability of lower stud depth thermal transmittance coefficients for higher stud depth assemblies for the range studied.

Table 4: Summary of predicted vs simulated heat flows

Spacing	R_{CI}	$\psi_{studs,\ 3.625}$	$\psi_{tracks,\ 3.625}$	$Q_{pred,\ 6.000}$	$Q_{Heat3\ 6.000}$	Δ
	m^2·K/W	W/m·K		W		%
407 mm (16 in)	No XPS	0.104	0.072	4.433	4.402	-0.7
	1.33	0.027	0.014	2.063	2.103	1.9
	1.77	0.020	0.011	1.776	1.806	1.6
	2.21	0.016	0.008	1.568	1.594	1.6
610 mm (24 in)	No XPS	0.102	0.075	3.920	3.895	-0.6
	1.33	0.026	0.016	1.932	1.961	1.5

9. Impact of external insulation

Addition of external insulation has drastic impact on overall heat flow through the wall assembly. 53% reduction in overall heat flow was observed when 1.33 m^2·K/W (R-7.5) external insulation was added to an assembly with no external insulation. Unlike localized mitigation solutions (Ex: rubber strips) the reduction of heat flow through the studs and tracks is nearly equal (73% and 79%) indicating that continuous insulation has a homogenous effect on mitigating thermal bridging.

Diminishing returns in reduction in heat flow are observed when additional cavity insulation is added. When CI is increased by 0.443 m^2·K/W (R-2.5) from 1.33 m^2·K/W (R-7.5) to 1.77 m^2·K/W (R-10), the reduction in overall heat flow is 14% for the studied assemblies. However, when CI is further increased by 0.443 m^2·K/W (R-2.5) to 2.21 m^2·K/W (R-12.5), heat flow through the planar wall, studs, and tracks decreases by 9%, 20% and 23% respectively to reduce the overall heat flow by 12 %. This observation is consistent with previously conducted studies by the authors [3]. Since heat flow is inversely proportional to assembly resistance, diminishing returns were expected when CI is increased.

Further, reductions in heat flow are approximately the same (53% and 51%) when comparing 407 mm (16 in) and 610 mm (24 in) on center assemblies. This indicates that impact of CI on wall assembly heat flow is independent of stud spacing for the studied range of spacings.

10. Summary of component level heat flows and thermal transmittance values

Component level heat flows and their respective thermal transmittance coefficients have been summarized in Table 5. Here, Q_{CW} and Q_{NA} are the heat flows through the wall assembly with and without thermal anomalies (CFS components) respectively. Further, Q_{studs} and Q_{tracks} are the heat flow through the studs and tracks and ψ_{studs} and ψ_{tracks} are the respective thermal transmittance coefficients calculated according to Equation 1 and Equation 2. These heat flow and thermal transmittance values were used to determine impact of CFS components, trends, and make predictions for heat flows that have been presented herein.

Table 5: Summary of heat flow and component level transmittance values

Assembly No.	Q_{CW}	Q_{NA}	Q_{Studs}	Q_{Tracks}	ψ_{studs}	ψ_{tracks}
	W				W/m·K	
1	4.478	2.293	1.770	0.358	0.104	0.072
2	2.085	1.522	0.457	0.071	0.027	0.014
3	1.794	1.374	0.344	0.052	0.020	0.011
4	1.583	1.250	0.274	0.041	0.016	0.008
5	4.402	2.306	1.694	0.343	0.099	0.069
6	2.103	1.534	0.466	0.072	0.027	0.014
7	1.806	1.380	0.348	0.053	0.020	0.011
8	1.594	1.254	0.278	0.041	0.016	0.008
9	3.949	2.293	1.242	0.373	0.102	0.075
10	1.946	1.529	0.317	0.081	0.026	0.016
11	3.895	2.306	1.187	0.360	0.097	0.073
12	1.961	1.534	0.324	0.081	0.027	0.016
13	4.181	2.292	1.506	0.319	0.088	0.064
14	4.565	2.306	1.834	0.357	0.107	0.072
15	4.692	2.292	1.943	0.368	0.114	0.074
16	4.909	2.292	2.132	0.385	0.125	0.078

11. Conclusions

CFS structural detailing has a significant impact on building envelope performance and accounting for thermal bridging at the design phase can improve the energy performance of CFS buildings. Based on the sixteen assemblies studied, the following key conclusions can be made: heat flow through the assembly increases non-linearly as member thickness is increased; CFS member spacing has a drastic impact on heat flow through the assembly but this impact is minimized when external CI is present; increasing stud depth has minimal impact on the thermal performance of wall assemblies; and, continuous insulation is effective, but there are diminishing returns in reduction of heat flow.

12. Acknowledgements

The writers gratefully acknowledge the financial support provided by the American Iron and Steel Institute (AISI) standards council. The writers also thank Jonathan Humble, Jay W. Larson, and Pat Ford for their technical suggestions and comments during this project.

References

[1] Martins, C., Santos, P., and Simoes da Silva, L. (2016). "Lightweight Steel-Framed Thermal Bridges Mitigation Strategies: A Parametric Study." Journal of Building Physics 39 (4): 342-372. doi:10.1177/1744259115572130

[2] AISI (American Iron and Steel Institute). (2018). "Thermal Analysis of Cold-Formed Steel Wall Assemblies". *AISI RP18-1*, Washington, DC.

[3] AISI (American Iron and Steel Institute). (2019). "Thermal Bridging in Cold-Formed Steel Wall Assemblies". *AISI RP19-2*, Washington, DC.

[4] ISO (International Organization for Standardization). (2007). "Thermal Bridges in Building Construction - Heat Flows and Surface Temperatures - Detailed Calculations," *ISO 10211*, Geneva, Switzerland.

[5] ASHRAE (American Society of Heating, Refrigerating and Air-Conditioning Engineers). (2016). "Energy Standard for Buildings Except Low-Rise Residential Buildings". *ASHRAE, Standard 90.1*, Atlanta, GA.

[6] Blomberg, T. (2017). "Heat 3 – A PC-program for heat transfer in three dimensions. Manual with brief theory and examples. Version 8.0" Dept. of Building Physics, Lund University, Lund, Sweden.

[7] ASHRAE (American Society of Heating, Refrigerating and Air-Conditioning Engineers). (2017). "Handbook of Fundamentals". *ASHRAE, HoF*, Atlanta, GA.

[8] ASHRAE (American Society of Heating, Refrigerating and Air-Conditioning Engineers). (1996). "Building Insulation System Thermal Anomalies". ASHRAE 785-RP, Atlanta, GA.

[9] ASHRAE (American Society of Heating, Refrigerating and Air-Conditioning Engineers). (2011). "Thermal Performance of Building Envelope Details for Mid - And High-Rise Buildings". ASHRAE 1365-RP, Atlanta, GA.

[10] Desjarlais, A., Biswas, K., Childs, P., and Atchley, J. (2012). "Compilation of Steady-State Hot Box Tests Conducted in 2011 and 2012 by Oak Ridge National Laboratory; Part 1 and Part 2.", ORNL, Oak Ridge, TN

Appendix

Table 6: Summary of nomenclature

NOMENCLATURE		
A	-	Area of Wall Assembly, m^2 (ft^2)
Q_{CW}	-	Overall heat flow through the wall assembly, W (BTU/hr)
Q_{Heat3}	-	Overall heat flow through the wall assembly from Heat 3, W (BTU/hr)
Q_{NA}	-	Net heat flow through the wall assembly without thermal anomalies, W (BTU/hr)
$Q_{No\ Studs}$	-	Heat flow through the wall assembly without Studs, W (BTU/hr)
Q_{pred}	-	Predicted heat flow through the wall assembly, W (BTU/hr)
R_{ins}	-	Thermal Resistance of cavity insulation, m·K/W, (hr·ft2°F/BTU-in)
R_{CI}	-	Thermal Resistance of continuous insulation, m·K/W, (hr·ft2°F/BTU-in)
T_e	-	Exterior temperature,°C (°F)
T_i	-	Interior temperature,°C (°F)
ψ	-	Linear thermal transmittance coefficient, W/m·K (BTU-in/hr·ft^2 °F)